

# Microfluidic Paper-Based Analytical Devices with Instrument-Free Detection and Miniaturized Portable Detectors

Takashi Kaneta,<sup>a</sup> Waleed Alhamad,<sup>b,c</sup> and Pakorn Varanusupakul<sup>b,c</sup>

<sup>a</sup>Department of Chemistry, Graduate School of Natural Science and Technology, Okayama University, Okayama, Japan

<sup>b</sup>Approaches for Food Applications Research Group, Faculty of Science, Chulalongkorn University, Bangkok, Thailand

<sup>c</sup>Department of Chemistry, Faculty of Science, Chulalongkorn University, Bangkok, Thailand

Address correspondence to Takashi Kaneta, Department of Chemistry, Graduate School of Natural Science and Technology, Okayama University, 3-1-1 Tsushimanaka, Okayama 700-8530, Japan

E-mail: kaneta@okayama-u.ac.jp

## ORCID

Takashi Kaneta: <http://orcid.org/0000-0001-9076-3906>

Waleed Alhamad: <http://orcid.org/0000-0003-1379-8755>

Pakorn Varanusupakul: <http://orcid.org/0000-0001-6374-7804>

Keywords: microfluidic paper-based analytical device, paper-based analytical device, point-of-care testing, onsite analysis

## ABSTRACT

Microfluidic paper-based analytical devices ( $\mu$ PADs) have attracted much attention over the past decade because they offer clinicians the ability to deliver point-of-care testing and onsite analysis. Many of the advantages of  $\mu$ PADs, however, are limited to work in a laboratory setting due to the difficulties of processing data when using electronic devices in the field. This review focuses on the use of  $\mu$ PADs that have the potential to work without batteries or with only small and portable devices such as smartphones, timers, or miniaturized detectors. The  $\mu$ PADs that can be operated without batteries are, in general, those that allow the visual judgment of analyte concentrations via readouts that are measured in time, distance, count, or text. Conversely, a smartphone works as a camera to permit the capture and processing of an image that digitizes the color intensity produced by the reaction of an analyte with a colorimetric reagent. Miniaturized detectors for electrochemical, fluorometric, chemiluminescence, and electrochemiluminescence methods are also discussed, although some of them require the use of a laptop computer for operation and data processing.

## Introduction

Much of modern analytical chemistry has recently moved in the direction of measuring analytes onsite rather than collecting samples at a targeted time and location for transport back to a central laboratory for subsequent analysis. Over the past decade, microfluidic paper-based analytical devices ( $\mu$ PADs or PADs) have demonstrated potential utility in point-of-care testing (POCT) and onsite analysis. A proof-of-principle report by the Whitesides group in 2007 (1) introduced the concept, and since then many groups have demonstrated applications for the analyses of biomolecules, metal ions, and inorganic anions. Many research groups have published comprehensive review articles on  $\mu$ PADs that provide a focused perspective and specific content. From the years 2013 to 2017, several groups published overviews of their research on  $\mu$ PADs (2-6). Conversely, many specific reviews have dealt with the fabrication of  $\mu$ PADs (7-9) and with detection methods that include electrochemistry (10-12), colorimetry (13,14), and electrochemiluminescence (15,16). Reviews of  $\mu$ PADs used for specific purposes such as environmental analysis (17,18), biochemical analysis, and POCT (19-24) have also been published. Other review articles have described topics such as the analyses of specific analytes (25,26), flow control (27), and energy applications (28).

These and many other articles on  $\mu$ PADs emphasize the advantages in POCT and onsite analysis due to low cost and portability. Many  $\mu$ PADs, however, remain far from practical for many of these purposes, and real applications in practical analysis are limited. Therefore, the present review is focused on the  $\mu$ PADs that actually show promise for applications to POCT and onsite analysis. To achieve analysis in the field,  $\mu$ PADs must be operated without the need for large instruments, which includes a heavy power supply.

Lateral flow assays (LFA) are important techniques in POCT, and many review articles of lateral flow immunoassays have been published since 2009 (29). More than 10 related

review articles have been published since 2015, although we cite only a few here (30-33). Investigations into LFA have focused mainly on practical applications to the semi-quantitative analyses of a target molecule rather than on methodological developments. Therefore, LFAs were not included in the present review in order to focus on the detection schemes of  $\mu$ PADs.

Here, we discuss instrument-free  $\mu$ PADs, miniaturized detectors, and otherwise handy types that are transportable, although a portion of them still require a laptop computer to act as a system controller, a data processor, and/or a power supply. Instrument-free  $\mu$ PADs employ readouts calibrated by time, distance, count, and/or text that are all, in principle, based on either colorimetry or fluorometry. By using smartphones and other small devices, miniaturized detection systems provide colorimetric, electrochemical, chemiluminescence, and electrochemiluminescence methods.

### **Instrument-Free Detection**

In the early studies of  $\mu$ PADs, colorimetry permitted the detection of analytes either qualitatively or semi-quantitatively by comparing the color intensity of a sample with those of standards (1). Both the amount and the concentration of an analyte can be determined semi-quantitatively via colorimetry using only the naked eye. Measuring an analyte quantitatively, however, requires images from  $\mu$ PADs that can be subjected to image processing. Therefore, quantitative analysis by  $\mu$ PADs based on colorimetry requires a digital camera or scanner to capture images and a PC for processing the images.

Digital cameras and PCs are transportable, but they are larger and heavier than  $\mu$ PADs for which portability and lightness are important advantages. Therefore, the preferred detector for onsite analysis is the naked human eye, which is actually quite sensitive to colors, but presents difficulties digitizing color intensities. To achieve quantitative

analysis by  $\mu$ PADs using only visual judgment, different research groups have developed methods of detection based on schemes that involve time, distance, count, or text.

Time-based detection was first developed by the Philips group (34). With this method, a  $\mu$ PAD with a timing readout produces a 3D structure that consists of stacked paper substrates (3D- $\mu$ PAD), as shown in Figure 1(A). The 3D- $\mu$ PAD consists of two flow channels, one is for negative control and the other maintains positive control. Each channel contains the substrate of a target enzyme, a phase-switching reagent that forms a hydrophobic barrier, and a dye that detects penetration of the sample solution. Glucose oxidase is immobilized on the bottom layer of the channel for positive control. In determining alkaline phosphatase (ALP), glucose-6-phosphate was added as the substrate. When a sample containing ALP was introduced into the 3D- $\mu$ PAD, glucose-6-phosphate was converted to glucose that was further oxidized by the immobilized glucose oxidase, and the result was  $\text{H}_2\text{O}_2$ . The produced  $\text{H}_2\text{O}_2$  cleaved the bonding of the phase-switching reagent, and made it hydrophilic. Therefore, the flow rate increased with increases in the concentration of  $\text{H}_2\text{O}_2$ , and the amount depended on the concentration of ALP in the sample solution. The timing readout of a 3D- $\mu$ PAD permitted the detection of ALP on a sub-picomolar level.

A similar strategy that used a timing readout was reported for the determination of  $\text{H}_2\text{O}_2$  and metal ions (35-37). Lewis et al. employed a timing readout for the determination of metal ions based on DNA cleavage in the presence of  $\text{Pb}^{2+}$  and a non-covalent complex formation of four polynucleotides in the presence of  $\text{Hg}^{2+}$  (36). Zhang et al. demonstrated the determination of  $\text{H}_2\text{O}_2$  via a catalytic reaction of 3',3',5',5'-tetramethylbenzidine (TMB) with horseradish peroxidase in the production of hydrophobic products (35). The hydrophobic products changed the wetting property of paper from hydrophilic to hydrophobic, so it subsequently prolonged the flow-through

time of the detection reagent. The Zhang group also used a timing readout to measure the potassium ion in a formation of hemin/G-quadruplex conjugates (37). A DNA probe binded with  $K^+$  and hemin molecules to form  $K^+$ -stabilized hemin/G-quadruplex conjugates. Subsequently, a peroxidase-like DNAzyme effectively catalyzed the  $H_2O_2$ -mediated oxidation of TMB to produce a highly hydrophobic poly-TMB product in the zone of the paper device. A blank sample (without  $K^+$ ), however, would not enable the production of poly-TMB in the zone. Therefore, the difference in the hydrophobicity of the reaction zone resulted in different flow-through times of the red ink solution, which acted as an indicator to detect the flowing solution. The flow-through time was positively correlated with the concentration of  $K^+$  in the sample.

A distance-based readout was first proposed by Cate et al. using precipitation reactions in a channel on a paper substrate (38). The fabrication, operation, and results are shown in Fig. 1(B). These results demonstrated measurements of glucose, nickel, and glutathione using three different forms of chemistry: an enzymatic reaction, a metal complexation, and a nanoparticle aggregation. Colorimetric reagents were deposited in a thermometer-like flow channel, and a sample solution was introduced into the channel. The colorimetric reagent reacted with an analyte to produce precipitation that formed a colored bar on the thermometer-like flow channel. The colored bar developed until the analyte in the sample solution was completely depleted. Distance-based detection has been applied to the simultaneous determinations of metal ions (39), lactoferrin (40), and DNA (41) wherein different detection schemes were employed for the analytes. Tian et al. published a comprehensive review of distance-based readouts in microfluidic devices, including  $\mu$ PADs, in 2016 (42).

Further applications of distance-based readouts were also reported in 2017 and 2018; the use of a  $\mu$ PAD for the analyses of DNAs (43, 44) and metal ions including copper (45),

mercury (46), and lead (47) was demonstrated using a distance-based readout. Piyanan et al. reported an antioxidant activity assay of nanoceria wherein antioxidants were used to partially reduce  $\text{Ce}^{4+}$  to  $\text{Ce}^{3+}$ , which resulted in a color change (48). Shimada et al. have significantly improved the sensitivity of distance-based  $\mu\text{PADs}$  in the determination of iron via the continuous flow of a sample solution (49). The limits of quantification were achieved at 28 ppb, which is comparable to that of inductively coupled plasma-optical emission spectrometry.

A counting-based readout was developed by Lewis et al. in the measurement of  $\text{H}_2\text{O}_2$  using a detection scheme similar to that of timing-based readouts where  $\text{H}_2\text{O}_2$  was used to convert hydrophobic chemicals to hydrophilic versions (50). Zhang et al. also demonstrated  $\text{H}_2\text{O}_2$  measurement using a counting-based readout wherein the oxidation of  $\text{I}^-$  to  $\text{I}_2$  generated a color change in the detection zone (35). Karita et al. employed a counting-based readout for acid-based titration (51) and chelation titration (52) using  $\mu\text{PADs}$  consisting of 10 reaction and detection zones located radially. The reaction zone contained different amounts of a titrant whereas a constant amount of an indicator was deposited in the detection zone. Therefore, a color change occurred either before or after the endpoint where the amount of the titrant was equivalent to that of the analyte. An example of the operation and the results are shown in Fig. 1 (C).

Yamada et al. demonstrated text readout using a transparent sheet, which acts as color filters that allow a color change to be judged by the naked eye (53). They employed a complex formation of albumin with tetrabromophenol blue (TBPB), which gradually changed the color from yellow to blue by combining with protein molecules. Text that indicated the concentrations of albumin were printed on a paper substrate using a TBPB solution as ink so that the text changed color depending on the concentration of albumin. The  $\mu\text{PAD}$  was covered by a transparent film with five different screening colors, and each

color corresponded to a concentration of the complex between TBPB and albumin. Therefore, when the color of the complex became more intense than the screening color, the text was displayed on the  $\mu$ PAD. The Yamada group listed the concentrations of proteins at 0.15, 0.3, 1, 3, and 10 mg mL<sup>-1</sup> using text-readout  $\mu$ PADs. A  $\mu$ PAD with a text-readout is shown in Fig. 1 (D). Other text-based devices have been reported, but these, in principle, represent only a semi-quantitative threshold amount of an analyte (54-56).

These readout detection schemes are completely instrument-free, which allows onsite analysis and POCT. Nevertheless, the demonstrations of onsite analysis or POCT have, in fact, been limited even though many articles have been published. The stability of reagents and the poor sensitivity of naked-eye detection warrant further investigation before onsite analysis and POCT can truly be considered practical.

### **Miniaturized Portable Detection Systems for $\mu$ PADs**

In many examples, researchers have designed miniaturized, portable, and handheld detection systems that can be readily carried to remote and outlying locations to measure, collect, and process data obtained from  $\mu$ PADs. These systems use various forms of input for detection: colorimetric, electrochemical, fluorescence, chemiluminescence, and electrochemiluminescence. In this section, we review miniaturized detection systems that digitize and/or process the results obtained onsite via  $\mu$ PADs.

#### ***Transmittance Colorimeter***

The most common analytical method for  $\mu$ PADs is colorimetry because it is relatively simple and the color intensity is proportional to analyte concentrations. Moreover, colorimetric detection is cost-effective and straightforward to operate with minimal



training. One of the simplest detectors in colorimetry is based on the measurement of transmittance, which is directly related to the absorbance of color generated by a chemical reaction. Ellerbee et al. introduced a handheld colorimetric detector that measures the transmission of light through paper, i.e., a portable transmittance colorimeter (57). The detector measures the transmittance of light passing through a  $\mu$ PAD where colors are developed. The  $\mu$ PAD is completely enclosed in the sensing area of an optical IC detector to prevent the penetration of stray light. The detector is equipped with a tricolor LED and an integrated switch to allow the user to select one of three illumination wavelengths. The light is pulsed and detected by kHz modulation with a narrow bandpass and frequency-sensitive detection to enable sensitive measurements in a variety of lighting conditions. Also, it is battery-operated and all the components (battery, detector, manifold, and substrate) are housed in an aluminum box ( $6.5 \times 14.7 \times 3.4$  cm), which reduces the weight of the detector and makes it easier to hand hold. A similar portable transmittance colorimeter has been employed for the colorimetric quantification of ascorbic acid (58). Swanson et al. reported another type of portable reader that could assess light transmittance in  $\mu$ PADs for the measurement of alanine aminotransferase, an indicator of liver health in blood (59). The handheld transmittance reader consists of two electrical circuit boards that drive a photodiode and LEDs, respectively. The electrical circuit boards measure the light transmittance of the  $\mu$ PAD when placed between the photodiode and LEDs fixed on individual boards. The portable reader has two operating modes: powered by a universal serial bus (USB) connection to a laptop computer and controlled using an accompanying desktop application, or powered from a battery while being operated independently with data stored in non-volatile memory for later retrieval.

Recently, Pogrebniak et al. introduced the first simple, miniaturized, and low-cost handheld transmittance detector based on a Paired-Emitter-Detector Diode (PEDD)

principle (60). This detector features only customary LEDs with no additional optical parts such as lenses, filters, or fibers. The first LED acts as a light emitter whereas the second is a detector that generates a photometric analytical signal directly proportional to the analyte concentration. A homemade low-voltage circuit based on a L272 chip is used for LED emitters powered by stable current, while LED detectors are connected to a handheld digital multimeter that functions as a voltmeter. This portable PEDD- $\mu$ PAD system can determine the amount of hemoglobin in human blood. In addition, the portable PEDD can be employed as a fluorescence detector because the LED acts as a partially selective light detector (60). Three types of transmittance colorimeters are summarized in Table 1.

### ***Image capturing and processing devices***

In general, quantitative analysis with colorimetry in  $\mu$ PADs requires the following steps: the capture of images, the processing of images, and the construction of a calibration curve. The most important issue for precise and accurate onsite measurements is to maintain a constant image capture since the color intensity of an image is sensitive to the spectrum and intensity of the light source.

Portable scanners (61,62) have been used as low-cost readers to capture images since the early stages of  $\mu$ PADs. The use of portable scanners to capture the color images of  $\mu$ PADs offers advantages that include a highly precise source of light, high resolution, and scanned images that are in focus mode. The scanned images are saved in JPEG format at 600 dpi (the most common resolution due to the acceptable size of images). The images undergo treatment by image processing software such as Adobe Photoshop® or ImageJ (63) that converts them to RGB (red, green, and blue) color intensities, CMYK (cyan (C), magenta (M), yellow (Y) and black or key (K)) (64), grey scale values (gray scale images

consist of combinations of black and white pixels), or HSV (Hue (H), saturation (S), values (V)) mode (65) in order to obtain and evaluate their colorimetric data. The values of color are proportional to the analyte concentrations, and each mode that corresponds to the changes in color intensity can be used to plot a calibration graph.

Jayawardane et al. (66) used a portable scanner coupled with a gas-diffusion  $\mu$ PAD for the onsite determination of ammonia in contaminated environmental water samples. In their work, the measured color intensity was converted to absorbance according to a method established by Birch and Stickle (67),  $\text{absorbance} = -\log(I/I_0)$ , where  $I$  is the mean for the color intensity of the sample or standard and  $I_0$  is the mean for the color intensity of the blank. However, it should be noted that portable scanners require an external power supply, although the power is usually obtained from the USB port of a personal computer.

Smartphone (or cell phone) cameras and digital cameras are optimal due to portability and advanced computing capabilities. A huge number of applications concerning the integration of smartphones (68-72) and digital cameras (73-75) with  $\mu$ PADs as an onsite detection platform have been published and reviewed. For the present review, we classified the applications into two categories according to the manner of image processing by smartphone cameras. In the first category, smartphones or digital cameras act only as image capture devices whereby the image files are transferred to desktop or laptop computers either via USB connector, Bluetooth, or via cloud computing for further processing in order to measure the mean for color intensity and to generate quantitative data (68,72,76-78). By comparison with portable scanners, cell phone cameras have disadvantages that involve the analytical features that are available. For example, sensitivity in a glucose assay obtained by a portable scanner is three times higher than that obtained by a cell phone camera. This is due to the illumination conditions that affect the intensities of digital images. Furthermore, cell phone cameras cannot provide

high-resolution images of small test areas because of the difficulty in focusing on a closed distance between the camera phone and a  $\mu$ PAD. In order to overcome and ameliorate these issues, researchers have used distinct hardware-to-device coupling strategies (79,80), the most common of which is the fabrication of a light-tight black box with LEDs to control the illumination conditions precisely and accurately (81-84).

In the second category, images are analyzed directly on a smartphone by using an application programmed specifically for image processing that results in complete onsite analysis of the samples (85-87). Ruiz et al. devised an android application for the simultaneous determinations of pH and nitrite concentration on  $\mu$ PADs (88). The application contains seven sensing zones that produce selective color changes. The flash of the smartphone is directly employed as a light source that can capture images in the dark. This application analyzes changes in the hue and saturation coordinates of the HSV color-sensing zones via an algorithm customized for image-processing. Results appear directly on the application screen. The reliability of the smartphone as a chemical detector to measure pH and nitrite concentrations has been validated. Moreover, Sicard and co-workers presented a smartphone application for the onsite colorimetric quantification of organophosphates in water samples (89). Their system consists of a  $\mu$ PAD and a smartphone equipped with a camera for capturing images. This system requires two  $\mu$ PADs for a single measurement; one tests a water sample and the other tests a clean water sample as a control.

Smartphones also permit the identification of the sampling locations via global positioning (GPS), which allows researchers to tag the analytical results with the locations on the map of a website. Moreover, in order to minimize the variations induced by lighting conditions, the images of control and test samples can be captured simultaneously side-by-side in a vertical position. Images consisting of both test and control  $\mu$ PADs can

guarantee the same lighting conditions and highly accurate measurements. On the other hand, dose-response curves to vary the concentrations of two types of pesticides have been plotted using both ImageJ and iPhone applications. The iPhone produced lower IC<sub>50</sub> values for two types of pesticides, and showed changes in intensity at lower pesticide concentrations, which was attributed to better detection limits. However, this application reports only the intensities of pixels as RGB values. In order to calculate the concentrations of samples, calibration curves must be plotted against the concentrations of an analyte.

As previously established, the three choices available for capturing the images of  $\mu$ PADs includes scanners, smartphones, and digital cameras, and the size decreases in the following order: scanner > digital camera  $\geq$  smartphone. Both the resolution and reproducibility of the scanner are the best. In addition, ambient light must be controlled to take images by digital cameras and smartphones since the images are sensitive to the illumination conditions. In terms of portability, however, smartphones show the most promise for onsite analysis because they can both capture images and process them.

### ***Electrochemical detection***

After colorimetry, electrochemistry, amperometry in particular, is the second most widely used method for  $\mu$ PADs. It is well known that electrochemical detection (ECD) has unique features that result in high sensitivity and high selectivity with the appropriate choice of detection potential and/or electrode material (90). The assays of ECD- $\mu$ PADs have been extensively explored due to small size, robustness, low cost, portability, miniaturization with digital readout, and simplicity of instrumentation (91,92).

As with traditional electrochemical systems, ECD assays on  $\mu$ PADs involve a three-electrode system that includes a working electrode, a counter electrode, and a

reference electrode. Henry and co-workers first reported the concept of electrochemical detection using  $\mu$ PADs, and referred to them as electrochemical microfluidic paper-based analytical devices (E $\mu$ PADs) (90). In their work, the working and counter electrodes were fabricated by printing carbon ink onto chromatographic paper, while the reference electrode and conductive pads were constructed from silver/silver chloride conductive ink. Screen printing is the most popular method currently being used to fabricate these electrodes on a paper substrate. Other electrode fabrication methods in E $\mu$ PADs include inkjet printing (93), pencil drawing (94), stencil printing (95), incorporating micro-wires as electrodes (96), and direct writing onto a paper surface using a pen (97).

In order to enhance the electrochemical signal and obtain lower limits of detection for E $\mu$ PADs, modifying electrodes with nanoparticles has become one of the most common strategies. Several methods to achieve this goal (98) have already been published, and the process continues to undergo development. For example, Nantaphol et al. (99) used a boron-doped diamond (BDD) working electrode modified with silver nanoparticles (AgNPs) to develop a  $\mu$ PAD that could sense cholesterol. A bare BDD electrode showed low sensitivity to  $\text{H}_2\text{O}_2$ , which was increased by the addition of AgNPs that have shown excellent electrocatalytic activity in  $\text{H}_2\text{O}_2$  reduction. In another example of a modified electrode, Rungsawang and coworkers developed an E $\mu$ PAD for the detection of glucose in human blood serum, soft drinks, apple juice, and sweet tea. They modified screen-printed carbon electrodes by mixing cellulose acetate with carbon ink and using 4-aminophenylboronic acid as a redox mediator to improve the sensitivity to glucose (100). It is noteworthy that some researchers have used gold as an alternative material for fabricating and modifying electrodes because of its excellent conductivity and unique features (101-104). For application to onsite analysis, however, all the E $\mu$ PADs mentioned here must use a transportable potentiostat for measurements and a laptop with

suitable software for the signal readout.

On the other hand, some research groups have developed E $\mu$ PADs for use with a handheld, portable device that can rapidly extract quantitative electrochemical readouts. The first attempt was by the Whitesides group (105). Their idea was based on combining E $\mu$ PADs with a commercial hand-held glucometer (Fig. 2 (A)) for the quantitative analysis of several analytes such as glucose, cholesterol, and lactate in human plasma or whole blood, and ethanol (or acetaldehyde) in water samples. The E $\mu$ PADs are fabricated on chromatography paper by means of wax printing. The E $\mu$ PADs consist of four electrodes (a working electrode, a counter electrode, and two internal reference electrodes) that are printed using graphite ink with wires and contact pads printed using silver ink. Wu et al. and Wang et al. integrated an E $\mu$ PAD with a commercial glucometer for the detection of ethanol and  $\beta$ -hydroxybutyrate (BHB) (106,107, respectively). The portable glucometers are convenient for electrochemical detection with E $\mu$ PADs.

A portable potentiostat for the electrochemical detection was fabricated in-house by Zhao and co-workers (108), as shown in Fig. 2 (B). This handheld potentiostat is combined with E $\mu$ PADs for the simultaneous determinations of glucose, lactate, and uric acid in urine samples. The E $\mu$ PADs contain eight bio-sensing modules; each module contains hydrophilic channels patterned with hydrophobic wax and three carbon electrodes screen-printed on the appropriate test zones. The contact pads are fabricated using silver strips. Detection is based on enzyme-catalyzed reactions, whereas the corresponding enzymes and electron-transfer mediators are stored in test zones. Unfortunately, a personal computer is needed to drive this portable potentiostat.

In order to make the potentiostat completely portable without a personal computer, a 3 V battery was integrated on a printed circuit board to power the circuit. Furthermore, smartphones have also been used in the development of electrochemical biosensors.

Fujimoto et al. developed a small, low-cost, and portable electrochemical biosensor consisting of a smartphone and an electrochemical biosensor device, as shown in Fig. 2(C) (109). The fabrication of this  $\mu$ PAD was accomplished by drawing three electrodes on chromatography paper using a carbon pencil (6B), while the pattern of the hydrophobic area was printed by a wax printer. The sensing device basically contains a complementary metal oxide semiconductor (COMS) chip. The CMOS chip has a USB that connects to a  $\mu$ PAD. Amperometric measurements are achieved using the iOS application developed by the Fujimoto group. The CMOS chip is connected to the earphone jack of a smartphone to apply a constant potential, which is controlled by adjusting the volume of the smartphone (iPod touch), to the electrodes on an  $\mu$ PAD. The output of the potentiostat, which corresponds to the current generated by the electrochemical reaction, is converted to a digital signal to be transmitted back to the iPod touch via microphone. The electrochemical biosensor for the  $\mu$ PAD measures glucose (109) and ethanol gas via coupling with enzymatic reactions (110).

Conversely, smartphones have the ability to receive data from other electronic devices via Bluetooth. This feature has been exploited by researchers to develop wireless electrochemical paper-based platforms and systems for different assays including amperometry and potentiometry (111-113). Fan et al. developed a wireless POCT system with electrochemical measurement for the onsite testing of neuron-specific enolase (NSE) (113). This system consists of a  $\mu$ PAD, an electrochemical detector, and a smartphone with an Android application. The  $\mu$ PAD uses a three-electrode system in which the working and counter electrodes are screen-printed with carbon ink while the reference electrode is screen-printed with Ag/AgCl ink. The surface of the working electrode is modified with nanocomposites synthesized by graphene functionalized with amino groups, thionine, and gold nanoparticles (NH<sub>2</sub>-G/Thi/AuNPs) for NSE detection. The



electrochemical detector consists of a potentiostat and a current-to-voltage converter powered either by a battery or USB port. Also, the detector is programmed with sweep voltage for generating a waveform for differential pulse voltammetry. The results are transmitted via Bluetooth from the detector to a smartphone, while Android applications working on smartphones were developed to record, display, and analyze the detection results of NSE. An example of the wireless electrochemical detector is shown in Fig. 2 (D).

### ***Fluorescence detection***

Fluorescence, chemiluminescence, and electrochemiluminescence forms of detection are intrinsically more sensitive than colorimetric detection because of the low background in the measurement of emitted light. Fluorescence  $\mu$ PAD assays involve fluorescence quenching-based detection (114,115) and fluorescence emission-based detection (116,117). To enhance the sensitivity of fluorescence  $\mu$ PAD assays, quantum dots are frequently embedded (118), immobilized (119), and printed (120) on paper. Also, fluorophores can be bound to the surface of paper (121,122).

As described in the section on colorimetry, Pogrebniak et al. (60) developed a low-cost PEDD for both photometric and fluorometric detection. The selection of LEDs depends on the excitation and emission maxima of the analyte, because the emission wavelengths of the LEDs for the excitation source and for the detector should be as close as possible to the excitation and emission maxima of the analyte, respectively. For example, fluorescein has an excitation maximum at 490 nm and an emission maximum at 521 nm; therefore, a blue (470 nm) LED would be selected for the excitation source with a red (630 nm) LED serving as the detector for fluorescence. Taudte et al. (123) developed a low-cost and portable fluorescence detector that uses  $\mu$ PADs to measure the level of

fluorescence quenching of pyrene by explosive compounds. Their detector consists of a UV-LED (365 nm) powered by a 3W battery and an ambient light photodiode sensor (500 nm). Under the optimized conditions, 10 different organic explosives including nitrate esters, nitro aromatics and nitro amines have been detected using the detector prototype with  $\mu$ PADs. The performance of the detector has been comparable to the bench-top instruments that were used to validate it.

Petruci et al. used a microfiber optic USB spectrometer instead of either a LED or a photodiode to develop a portable, online fluorescence detector with a disposable paper-based gas sensor platform for the *in-situ* determination of gaseous hydrogen sulfide (124) that uses a LED (470 nm) as the excitation source. The determination of H<sub>2</sub>S was based on the fluorescence quenching of fluorescein mercury acetate (FMA) by H<sub>2</sub>S gas. One main advantage of the detector is a short response time (60 s), which enables its use in rapid-analysis applications, and gives it the ability to detect small changes in the background of H<sub>2</sub>S concentrations.

One of the earlier examples of a digital camera in fluorescence measurements was reported by Petryayeva et al. (125) for the determination of peptides based on Förster resonance energy transfer (FRET). First, they immobilized semiconductor quantum dots (QDs) on paper substrates, which were then incubated with a dye-labeled peptide substrate in the same positions to generate an efficient FRET. While LED light (405 nm) excited the QDs, the images were captured by a digital camera and analyzed on the basis of the red/green color intensity ratio.

A recent paper by Guzman and co-workers (126) highlights the advantages of using a low-cost CMOS camera with a  $\mu$ PAD for onsite fluorescence measurements. They described the development of an integrated platform, which consists of a  $\mu$ PAD and a portable detection system comprised of a power source, a UV-LED, a chip holder, a hot

plate, a CMOS camera, and a smartphone, which can be used for the determination of formaldehyde at low concentrations. The detection of formaldehyde was based on a Hantzsch reaction. Briefly, the reaction zone of the  $\mu$ PAD is coated with ammonium acetate and acetoacetanilide (AAA). After dropping a formaldehyde solution onto the reaction zone of the  $\mu$ PAD and illuminating it with a LED light, the resultant fluorescent complex of AAA and formaldehyde is observed via a CMOS camera, and the digital image is transferred via connection to a smartphone with RGB color analysis software installed for the quantitative measurement of formaldehyde.

Smartphones are frequently equipped with efficient sensors, high-quality cameras, and computational ability. These features have been used as miniaturized and portable analytical tools in fluorescence measurements to capture fluorescent responses and quantify the assays in different fields incorporated with  $\mu$ PADs, whereas the captured images are analyzed using image-processing software to measure the RGB or gray values (127,128).

Recently, Song et al. (128) developed a portable and cost-effective device for online preconcentration fluorescent whitening agents. The system consists of a  $\mu$ PAD, UV-LED, macro-focusing lens, smartphone, and a miniaturized DC voltage source. The main idea of their work was to enhance  $\mu$ PAD performance with electrokinetic stacking and to use a smartphone as a fluorescence image detector. The acquired images are processed by ImageJ software to measure the gray values. The developed system shows a limit of detection (LOD) (0.06  $\mu\text{g/mL}$ ) that would approximate that (0.013  $\mu\text{g/mL}$ ) achieved by a desktop fluorescent spectrophotometer, which was used instead of a smartphone to measure the fluorescence.

### ***Chemiluminescence and electrochemiluminescence detection***

Chemiluminescence (CL) sensors measure the light intensity (the photon emission) generated by the chemical reactions of two reactants in the presence of a catalyst or an excited intermediate. Compared with fluorescence-based sensors, CL-based sensors require no external light sources, which is advantageous because it decreases the background noise and miniaturizes the detector. Because of high sensitivity, a wide dynamic range, and a low cost, CL is very attractive to researchers as a sensitive and efficient detection technique for  $\mu$ PADs. Alhamad et al. (129) developed a miniaturized chemiluminescence detection system for the determination of Cr (III) in water samples. The system consists of a  $\mu$ PAD, a small photomultiplier tube module (22×22×60 mm), a power supply operated at 1.2V, and a holder made of dark black acrylic for the  $\mu$ PAD. The novelty of their work lies in their  $\mu$ PAD design as well as in the holder. Each  $\mu$ PAD consists of 6 channels that allow the determination of 6 different samples in succession. Each channel is composed of an injection zone, a reaction zone, and a waste zone. The  $\mu$ PAD can generate signals with a peaked shape by fabricating an additional waste zone that has preventing too much of the reagent from staying in the reaction zone. Moreover, the holder is equipped with 6 optical fibers that connect the reaction zone to a photomultiplier tube in order to achieve 6 successive measurements of the samples and standards. In their work, 6 sequential injections were completed within 1 min for each  $\mu$ PAD, which resulted in a short analysis time and high throughput.

An inexpensive charge-coupled device (CCD) camera served as the detector for a CL- $\mu$ PAD assay that was first developed by Liu et al. (130) in the detection of 198-bp DNA fragments. The developed system detects long DNA amplicons on the basis of hybridization reactions with a covalently immobilized DNA probe and strands of biotin-labeled signal DNA. Under their optimal conditions, the LOD was 3 to 5 orders of magnitude lower than those obtained from other CCD-based microfluidic CL DNA assays.

The use of digital cameras and smartphones as low-cost and reliable readout tools has been successfully combined with CL- $\mu$ PADs for several applications in analytical fields, such as the detection of  $\text{H}_2\text{O}_2$  in biological samples (131) and salivary cortisol (132). Spyrou et al. (133) demonstrated the advantages of using a digital camera and a smartphone as detectors for CL- $\mu$ PAD assays. They developed a method for the chemiluminometric genotyping of a C677T single-nucleotide polymorphism (SNP). In order to detect the emerging chemiluminescence from the sensing areas, the authors constructed a 3D-printed smartphone attachment that houses inexpensive lenses that helps convert the smartphone into a portable chemiluminescence imager. Their work highlighted the ability to discriminate two alleles of a SNP in a single shot by imaging the strip, which avoided the need for dual labeling.

As an alternative to  $\mu$ PAD assays (134), electro-generated chemiluminescence (ECL) depends on electrochemical reactions to generate luminescence. The most common ECL reagents are tris(bipyridine)-ruthenium(II) ( $\text{Ru}(\text{bpy})_3^{2+}$ ) and luminol. The advantages of ECL over CL include low background signals and selectivity that is enhanced by controlling the electrode potential, but a potentiostat is required.

In 2010, Delaney et al. (135) used a mobile phone camera to capture images of ECL emissions on a  $\mu$ PAD for the determination of 2-(dibutylamino)-ethanol (DBAE) and nicotinamide adenine dinucleotide (NADH). The images were analyzed using a program called “Python” that separates the pixels into red, green, and blue values. Their method could detect DBAE and NADH at levels of 0.9  $\mu\text{M}$  and 72  $\mu\text{M}$ , respectively. Mani et al. used a CCD camera to measure ECL light in onsite environmental monitoring (136). In their work, the images from  $\mu$ PADs were processed using Gene Snap software that was converted to a color scale via Adobe Photoshop. Their method was successfully applied to measuring the presence of genotoxic equivalents in environmental samples. In another

example, Doeven and co-workers (137) developed a new strategy for multiplexed ECL detection for low-cost, portable clinical diagnostic devices that utilize a digital camera as the detector. Theirs was the first demonstration of red, green and blue (RGB) emitters effectively resolved using distinct applied potentials. Thus, the RGB values of the ECL intensity versus applied-potential curves could be effectively isolated to a single emitter at each potential. The ECL images captured by a camera were analyzed by ImageJ software; the mean RGB values were measured using the “Measure – RGB Values” function built into ImageJ.

In all the examples, however, the authors relied on the use of expensive potentiostats to generate the applied electrode potential, which underscores a critical problem for ECL detection when cost and portability are required. To overcome this problem, Delaney and co-workers (138) applied the electrode potential from the audio socket of a mobile phone by using suitable software (a Java-based application written for Android devices) that served the basic function of a potentiostat, which is to control an applied potential in order to initiate an electrochemical reaction. The maximum output voltage was 1.77 V. The application initiated an ECL reaction by playing an audio file containing a generated square waveform that consisted of a 100 ms positive interval and a 40 ms negative interval. Meanwhile, the ECL signal intensity was captured using the same application with the camera in video mode at a resolution of 320×240 pixels and approximately 30 fps. The total red intensity from the RGB channel was proportional to the analyte concentrations, and was extracted in real time from these images. The maximum output voltage was approximately 1.77 V which was sufficient to generate ECL from the  $\text{Ru}(\text{bpy})_3^{2+}$ /co-reactant system.

Recently, Chen et al. (139) developed a hand-held paper-based bipolar electrode-electrochemiluminescence (P-BPE-ECL) system for portable biochemical

analysis at the point-of-care level. The system uses a rechargeable battery as a power supply, an electronic circuit for voltage control, a smartphone as a detector for the ECL signal, a  $\mu$ PAD, and an instrument container. For the P-BPE-ECL system, the carbon ink-based BPE and driving electrodes are screen-printed on a paper substrate. The images are captured with a smartphone and wirelessly transmitted to a personal computer. The images are processed using ImageJ software, which converts the brightness of each pixel on the micrograph to photon counts. The authors highlighted several attractive features of the P-BPE-ECL system, the most important of which is that the P-BPE-ECL device requires only a low level of driving voltage, and the total energy-consumption is small. Furthermore, the P-BPE-ECL system has been successfully applied to the determination of  $\text{H}_2\text{O}_2$  and the detection of glucose in different samples within acceptable levels for sensitivity, dynamic range, stability, and reproducibility. Moreover, this system has the potential for high-throughput glucose screening.

### ***Other detection methods***

In place of large-scale equipment, portable surface-enhanced Raman spectroscopy (SERS) was recently integrated into  $\mu$ PADs for onsite analysis due to ease of operation, rapidity, specificity, and high sensitivity. Chen et al. (140) developed a portable sensor for the onsite determination of sulfites in wine. The sensor consists of a gas-diffusion  $\mu$ PAD with a portable Raman spectrometer for SERS. The gas-diffusion  $\mu$ PAD was fabricated by assembling layers of patterned filter paper containing a hydrophilic sample zone impregnated with a sulfuric acid solution followed by a PTFE hydrophobic microporous membrane layer and finally by a ZnO paper disc. The resultant  $\mu$ PAD was laminated to maintain the alignment of these layers. The novelty of the  $\mu$ PAD is the ability to separate and preconcentrate gas on a paper-based platform. In another example,

Villa and his co-worker developed a quantitative method for the onsite determination of uric acid in urine by using a portable Raman spectrometer combined with a paper-based substrate coated with gold nanoparticles (141).

In addition to the known and traditional analytical instruments, a wearable technology, the Google Glass, has been developed. Feng et al. (142) used the Google Glass for qualitative and quantitative measurements of lateral flow assays. More accurately, they used it for qualitative human immunodeficiency virus testing and for quantitative prostate-specific antigen testing. The main features of this platform are as follows: hands-free, voice-controlled interface, storage of information on a centralized server, detecting and processing multiple targets imaged using the Google Glass built-in camera under natural illumination conditions, and real-time spatio-temporal tracking of various diseases and personal medical conditions.

## **Conclusions**

We have reviewed  $\mu$ PADs that are portable with readouts intended for validation using only the naked eye. These portable detectors have been developed for different types of applications due to the advent of new materials and technologies. As this review shows, smartphones play many roles in detection systems ranging from optical to electrochemical due to unique features that include high-quality camera lenses, processing ability, input and output signaling, and the ability to transmit data to other devices. Obviously, the performance of smartphones is approaching that of personal computers, and in many cases smartphones are already replacing personal computers. Compared with electrochemistry and luminescence detection systems, colorimetric detectors require no special attachments such as potentiostats and excitation light sources, which has simplified their use in a variety of research areas. On the other hand, all-in-one detection devices (108,110,113)



have the advantage of being fully portable systems for most applications that require a portable potentiostat such as electrochemical detection, in particular. However, major challenges for these detectors include LODs as well as area coverage, particularly in POCTs. We hope that insight from our review will inspire readers to develop more portable and miniaturized detection methods in all research fields.

## Acknowledgments

This research was supported by JSPS KAKENHI Grant Number 17H05465. W. A. thanks the Rachadapisek Sompot Fund for a Postdoctoral Fellowship, Chulalongkorn University.

## References

1. Martinez, A. W., Phillips, S. T., Butte, M. J., and Whitesides G. M. (2007) Patterned paper as a platform for inexpensive, low-volume, portable bioassays. *Angew. Chem. Int. Ed.*, 46: 1318 –1320.
2. Lisowski, P. and Zarzycki, P. K. (2013) Microfluidic paper-based analytical devices ( $\mu$ PADs) and micro total analysis systems ( $\mu$ TAS): Development, applications and future trends. *Chromatographia*, 76: 19–20.
3. Nery, E. W. and Kubota, L. T. (2013) Sensing approaches on paper-based devices: A review. *Anal. Bioanal. Chem.*, 405: 7573–7595.
4. Cate, D. M., Adkins, J. A., Mettakoonpitak, J., and Henry, C. S. (2015) Recent developments in paper-based microfluidic devices. *Anal. Chem.*, 87: 19–41.
5. Yang, Y., Noviana, E., Nguyen, M. P., Geiss, B. J., Dandy, D. S., and Henry, C. S. (2017) Paper-based microfluidic devices: Emerging themes and applications. *Anal. Chem.*, 89:

71–91.

6. Yamada, K., Shibata, H., Suzuki, K., and Citterio, D. (2017) Toward practical application of paper-based microfluidics for medical diagnostics: State-of-the-art and challenges. *Lab Chip*, 17: 1206–1249
7. Sher, M., Zhuang, R., Demirci, U., and Asghar, W. (2017) Paper-based analytical devices for clinical diagnosis: recent advances in the fabrication techniques and sensing mechanisms. *Expert Rev. Mol. Diagn.*, 17: 351–366.
8. He, Y., Wu, Y., Fu, J. Z., and Wu, W. B. (2015) Fabrication of paper-based microfluidic analysis devices: A review. *RSC Adv.*, 5: 78109–78127.
9. Yamada, K., Henares, T. G., Suzuki, K., and Citterio, D. (2015) Paper-based inkjet-printed microfluidic analytical devices, *Angew. Chem. Int. Ed.*, 54: 5294–5310.
10. Adkins, J., Boehle, K., and Henry, C. (2015) Electrochemical paper-based microfluidic devices. *Electroporesis*, 36: 1811–1824.
11. Oh, J.-M. and Chow, K.-F. (2015) Recent developments in electrochemical paper-based analytical devices. *Anal. Methods*, 7: 7951–7960.
12. Mettakoonpitak, J., Boehle, K., Nantaphol, S., Teengam, P., Adkins, J. A., Srisa-Art, M., and Henry, C. S. (2016) Electrochemistry on paper-based analytical devices: A review. *Electroanalysis*, 28: 1420–1436.
13. Yao, B., Zhang, J., Kou, T. Y., Song, Y., Liu, T. Y., and Li, Y. (2017) Paper-based electrodes for flexible energy storage devices. *Adv. Sci.*, 4: 1700107.
14. Sriram, G, Bhat, M. P., Patil, P., Uthappa, U. T., Jung, H. Y., Altalhi, T., Kumeria, T., Aminabhavi, T. M., Pai, R. K., Madhuprasad, and Kurkuri, M. D. (2017) Paper-based microfluidic analytical devices for colorimetric detection of toxic ions: A review, *Trends Anal. Chem.*, 93: 212–227.
15. Morbioli, G. G., Mazzu-Nascimento, T., Stockton, A. M., and Carrilho, E. (2017)

Technical aspects and challenges of colorimetric detection with microfluidic paper-based analytical devices ( $\mu$ PADs) - A review. *Anal. Chim. Acta*, 970: 1–22.

16. L., Yu, J. H., Ge, S. G., and Yan, M. (2014) Lab-on-paper-based devices using chemiluminescence and electrogenerated chemiluminescence detection. *Anal. Bioanal. Chem.*, 406: 5613–5630.

17 Gross, E. M., Durant, H. E., Hipp, K. N., and Lai, R. Y. (2017) Electrochemiluminescence detection in paper-based and other inexpensive microfluidic devices. *ChemElectroChem*, 4: 1594–1603.

18. Busa, L. S. A., Mohammadi, S., Maeki, M., Ishida, A., Tani, H., and Tokeshi, M. (2016) Advances in microfluidic paper-based analytical devices for food and water analysis. *Micromachines*, 7: 86.

19. Meredith, N. A., Quinn, C., Cate, D. M., Reilly, T. H., Volckens, J., and Henry, C. S. (2016) Paper-based analytical devices for environmental analysis. *Analyst*, 141: 1874–1887.

20. Yetisen, A. K., Akram, M. S., and Lowe, C. R. (2013) Paper-based microfluidic point-of-care diagnostic devices. *Lab Chip*, 13: 2210 –2251.

21. Jeong, S.-G., Kim, J., Nam, J.-O., Song Y. S., and Lee C.-S. (2013) Paper-based analytical device for quantitative urinalysis. *Int. Neurourol. J.*, 17: 155–161.

22. Santhiago, M., Nery, E. W., Santos, G. P., and Kubota, L. T. (2014) Microfluidic paper-based devices for bioanalytical applications. *Bioanalysis*, 6: 89–106.

23. Rozand, C. (2014) Paper-based analytical devices for point-of-care infectious disease testing. *Eur. J. Clin. Microbiol. Infect. Dis.*, 33: 147–156.

24. Xia, Y., Si, J., and Li, Z. (2016) Fabrication techniques for microfluidic paper-based analytical devices and their applications for biological testing: A review. *Biosens. Bioelectron.*, 77: 774–789.

25. Lim, W. Y., Goh, B. T., and Khor, S. M. (2017) Microfluidic paper-based analytical devices for potential use in quantitative and direct detection of disease biomarkers in clinical analysis. *J. Chromatogr. B*, 1060: 424442.
26. Briquaire, R., Colwell, R. R., Boncy, J., Rossignol, E., Dardy, A., Pandini, I., Villeval, F., Machuron, J.-L., Huq, A., and Rashed, S. (2017) Application of a paper based device containing a new culture medium to detect *Vibrio cholerae* in water samples collected in Haiti. *J. Microbiol. Methods*, 133: 23–31.
27. Liu, S., Su, W., and Ding, X. (2016) A review on microfluidic paper-based analytical devices for glucose detection. *Sensors*, 16: 2086.
28. Jeong, S.-G., Kim, J., Jin, S. H., Park, K.-S., and Lee, C.-S. (2016) Flow control in paper-based microfluidic device for automatic multistep assays: A focused minireview. *Korean J. Chem. Eng.*, 33: 2761–2770.
29. Sharifi, F., Ghobadian, S., Cavalcanti, F. R., and Hashemi, N. (2015) Paper-based devices for energy applications. *Renew. Sust. Energ. Rev.*, 52: 1453–1472.
30. Posthuma-Trumpie, G. A., Korf, J., and van Amerongen, A. (2009) Lateral flow (immuno)assay: its strengths, weaknesses, opportunities and threats. A literature survey, *Anal. Bioanal. Chem.*, 393:569–582
31. Quesada-Gonzalez, D. and Merkoci, A., (2015) Nanoparticle-based lateral flow biosensors, *Biosens. Bioelectron.*, 73, 47–63
32. Eltzov, E., Guttel, S., Kei, A. L. Y., Sinawang, P. D., Ionescu, R. E., and Marks, R. S., (2015) Lateral flow immunoassays - from paper strip to smartphone technology, *Electroanalysis*, 27, 2116–2130.
33. Bahadir, E. B. and Sezginturk, M. K. (2016) Lateral flow assays: Principles, designs and labels, *Trends Anal. Chem.*, 82: 286–306.
34. Lewis, G. G., Robbins, J. S., and Phillips, S. T. (2013) Point-of-care assay platform for

quantifying active enzymes to femtomolar levels using measurements of time as the readout, *Anal. Chem.*, 85: 10432–10439.

35. Zhang, Y., Zhou, C., Nie, J., Le, S., Qin, Q., Liu, F., Li, Y., and Li, J., (2014) Equipment-free quantitative measurement for microfluidic paper-based analytical devices fabricated using the principles of movable-type printing, *Anal. Chem.*, 86, 2005–2012.

36. Lewis, G. G., Robbins, J. S., and Phillips, S. T. (2014) A prototype point-of-use assay for measuring heavy metal contamination in water using time as a quantitative readout, *Chem. Commun.*, 50: 5352–5354.

37. Zhang, Y., Fan, J., Nie, J., Le, S., Zhu, W., Gao, D., Yang, J., Zhang, S., and Li, J., (2015) Timing readout in paper device for quantitative point-of-use hemin/G-quadruplex DNAzyme-based bioassays, *Biosens. Bioelectron.*, 73: 13–18.

38. Cate, D. M., Dungchai, W., Cunningham, J. C., Volckens, J., and Henry, C. S., (2013) Simple, distance-based measurement for paper analytical devices, *Lab Chip*, 13, 2397–2404.

39. Cate, D. M., Noblitt S. D., Volckens, J., and Henry, C. S., (2015) Multiplexed paper analytical device for quantification of metals using distance-based detection, *Lab Chip*, 15, 2808–2818.

40. Yamada, K. Henares, T. G., Suzuki, K., and Citterio, D., (2015) Distance-based tear lactoferrin assay on microfluidic paper device using interfacial interactions on surface-modified cellulose, *ACS Appl. Mater. Interfaces*, 7, 24864–24875.

41. Wei, X. F., Tian, T., Jia, S. S., Zhu, Z., Ma, Y. L., Sun, J. J., Lin, Z. Y., and Yang, C. J., (2016) Microfluidic distance readout sweet hydrogel integrated paper-based analytical device ( $\mu$ DiSH-PAD) for visual quantitative point-of-care testing, *Anal. Chem.*, 88, 2345–2352.

42. Tian, T., Li, J., Song, Y., Zhou, L., Zhu Z., and Yang, C. J. (2016) Distance-based

microfluidic quantitative detection methods for point-of-care testing, *Lab Chip*, 16, 1139–1151.

43. Tian, T., An, Y., Wu, Y. Song, Y., Zhu Z., and Yang, C. (2017) Integrated distance-based origami paper analytical device for one-step visualized analysis, *ACS Appl. Mater. Interfaces*, 9, 30480–30487

44. Hongwarittorn, I., Chaichanawongsaroj N., and Laiwattanapaisa W. (2017) Semi-quantitative visual detection of loop mediated isothermal amplification (LAMP)-generated DNA by distance-based measurement on a paper device, *Talanta*, 175, 135–142.

45. Pratiwia, R., Nguyend, M. P., Ibrahima, S., Yoshioka, N., Henry, C. S., and Tjahjono, D. H. (2017) A selective distance-based paper analytical device for copper(II) determination using a porphyrin derivative, *Talanta*, 174, 493–499.

46. Cai, L., Fang, Y., Mo, Y., Huang, Y., Xu, C., Zhang, Z., and Wang, M. (2017) Visual quantification of Hg on a microfluidic paper-based analytical device using distance-based detection technique, *AIP Adv.*, 7, 085214.

47. Buring, S., Saetear, P., Tiyaongpattana, W., Uraisin, K., Wilairat, P., Nacapricha, D., and Ratanawimarnwong, N., (2018) Microfluidic paper-based analytical device for quantification of lead using reaction band-length for identification of bullet hole and its potential for estimating firing distance, *Anal. Sci.*, 34, 83–89.

48. Piyanan, T., Athipornchai, A., Henry, C. S., and Sameenoi, Y., (2018) An instrument-free detection of antioxidant activity using paper-based analytical devices coated with nanoceria, *Anal. Sci.*, 34, 97–102.

49. Shimada, Y. and Kaneta, T., (2018) Highly sensitive paper-based analytical devices with the introduction of a large-volume sample via continuous flow, *Anal. Sci.*, 34, 65–70.

50. Lewis, G. G., DiTucci, M. J., and Phillips, S. T. (2012) Quantifying analytes in

paper-based microfluidic devices without using external electronic readers, *Angew. Chem. Int. Ed.*, 124, 12879–12882.

51. Karita, S. and Kaneta, T. (2014) Acid-base titrations using microfluidic paper-based analytical devices, *Anal. Chem.*, 86, 12108–12114.

52. Karita, S. and Kaneta, T. (2016) Chelate titrations of  $\text{Ca}^{2+}$  and  $\text{Mg}^{2+}$  using microfluidic paper-based analytical devices, *Anal. Chim. Acta*, 924, 60–67.

53. Yamada, K., Suzuki, K., and Citterio, D. (2017) Text-displaying colorimetric paper-based analytical device, *ACS Sens.*, 2, 1247–1254.

54. Li, M., Tian, J., Al-Tamimi, M., and Shen W. (2012) Paper-based blood typing device that reports patient's blood type "in writing", *Angew. Chem. Int. Ed.*, 51, 5497–5501.

55. Carrasquilla, C., Little, J. R. L., Li, Y., and Brennan, J. D. (2015) Patterned paper sensors printed with long-chain DNA aptamers, *Chem. Eur. J.*, 21, 7369–7373.

56. Chen, X., Yu, S., Yang, L., Wang J., and Jiang C. (2016) Fluorescence and visual detection of fluoride ions using a photoluminescent graphene oxide paper sensor, *Nanoscale*, 8, 13669–13677.

57. Ellerbee, A. K., Phillips, S. T., Siegel, A. C., Mirica, K. A., Martinez, A. W., Striehl, P., Jain, N., Prentiss, M., and Whitesides, G. M. (2009) Quantifying colorimetric assays in paper-based microfluidic devices by measuring the transmission of light through paper. *Anal. Chem.*, 81: 8447–8452.

58. Ferreira, D. C. M., Giordano, G. F., Soares, C. C. D. P., de Oliveira, J. F. A., Mendes, R. K., Piazzetta, M. H., Gobbi, A. L., and Cardoso, M. B. (2015) Optical paper-based sensor for ascorbic acid quantification using silver nanoparticles. *Talanta*, 141:188–194.

59. Swanson, C., Lee, S., Aranyosi, A. J., Tien, B., Chan, C., Wong, M., Lowe, J., Jain, S., and Ghaffari, R. (2015) Rapid light transmittance measurements in paper-based microfluidic devices. *Sens. and Bio-Sens. Research*, 5:55–61.

60. Fiedoruk-Pogrebniak, M., Granica, M., and Koncki, R. (2018) Compact detectors made of paired leds for photometric and fluorometric measurements on paper. *Talanta*, 178:31–36.
61. Yang, X., Piety, N. Z., Vignes, S. M., Benton, M. S., Kanter, J., and Shevkoplyas, S. S. (2013) Simple paper-based test for measuring blood hemoglobin concentration in resource-limited settings. *Clin. Chem.*, 59:1506–1513.
62. Martinez, A. W., Phillips, S. T., Carrilho, E., Thomas III, S. W., Sindi, H., and Whitesides, G. M. (2008) Simple telemedicine for developing regions: Camera phones and paper-based microfluidic devices for real-time, off-site diagnosis. *Anal. Chem.*, 80:3699–3707.
63. Rasband, W.S. ImageJ, U. S. National Institutes of Health, Bethesda, Maryland, USA, <https://imagej.nih.gov/ij/>, 1997-2016.
64. Burger, W., and Burge, M. J. (2009) Principles of digital image processing. *Fundamental techniques*. Springer, London.
65. Sharma, G. (2002) Digital color imaging handbook. CRC Press, Boca Raton, London, New York, Washington, D.C..
66. Jayawardane, B. M., Mckelvie, I. D., and Kolev, S. D. (2015) Development of a gas-diffusion microfluidic paper-based analytical device ( $\mu$ PAD) for the determination of ammonia in wastewater samples. *Anal. Chem.*, 87 (9):4621–4626.
67. Birch, N. C., and Stickle, D. F. (2003) Example of use of a desktop scanner for data acquisition in a colorimetric assay. *Clin. Chim. Acta*, 333 (1):95–96.
68. Grudpan, K., Kolev, S. D., Lapanantnopakhun, S., Mckelvie, I. D., and Wongwilai, W. (2015) Applications of everyday it and communications devices in modern analytical chemistry: A review. *Talanta*, 136:84–94.



69. Zhang, D. and Liu, Q. (2016) Biosensors and bioelectronics on smartphone for portable biochemical detection. *Biosens. Bioelectron.*, 75:273–284.
70. Lopez-Marzo, A. M. and Merkoci, A. (2016) Paper-based sensors and assays: A success of the engineering design and the convergence of knowledge areas. *Lab Chip*, 16:3150–3176.
71. Roda, A., Michelini, E., Zangheri, M., Di Fusco, M., Calabria, D., and Simoni, P. (2016) Smartphone-based biosensors: A critical review and perspectives. *Trends Anal. Chem.*, 79:317–325.
72. Morbioli, G. G., Mazzu-Nascimento, T., Stockton, A. M., and Carrilho, E. (2017) Technical aspects and challenges of colorimetric detection with microfluidic paper-based analytical devices ( $\mu$ PADs) - a review. *Anal. Chim. Acta*, 970:1–22.
73. Komatsu, T., Mohammadi, S., Busa, L. S., Maeki, M., Ishida, A., Tani, H., and Tokeshi, M. (2016) Image analysis for a microfluidic paper-based analytical device using the CIE  $L^*a^*b^*$  color system. *Analyst*, 141:6507–6509.
74. Phansi, P., Sumantakul, S., Wongpakdee, T., Fukana, N., Ratanawimarnwong, N., Sitanurak, J., and Nacapricha, D. (2016) Membraneless gas-separation microfluidic paper-based analytical devices for direct quantitation of volatile and nonvolatile compounds. *Anal. Chem.*, 88:8749–8756.
75. Satarpai, T., Shiowatana, J., and Siripinyanond, A. (2016) Paper-based analytical device for sampling, on-site preconcentration and detection of ppb lead in water. *Talanta*, 154:504–510.
76. Choodum, A., Kanatharana, P., Wongniramaikul, W., and Daeid, N. N. (2013) Using the iphone as a device for a rapid quantitative analysis of trinitrotoluene in soil. *Talanta*, 115:143–149.

77. Chen, G. H., Chen, W. Y., Yen, Y. C., Wang, C. W., Chang, H. T., and Chen, C. F. (2014) Detection of mercury(II) ions using colorimetric gold nanoparticles on paper-based analytical devices. *Anal. Chem.*, 86 (14):6843–6849.
78. Songjaroen, T., Dungchai, W., Chailapakul, O., and Laiwattanapaisal, W. (2011) Novel, simple and low-cost alternative method for fabrication of paper-based microfluidics by wax dipping. *Talanta*, 85:2587–2593.
79. Chun, H. J., Park, Y. M., Han, Y. D., Jang, Y. H., and Yoon, H. C. (2014) Paper-based glucose biosensing system utilizing a smartphone as a signal reader. *BioChip J.*, 8:218–226.
80. Oncescu, V., O'dell, D., and Erickson, D. (2013) Smartphone based health accessory for colorimetric detection of biomarkers in sweat and saliva. *Lab Chip*, 13:3232–3238.
81. Meelapsom, R., Jarujamrus, P., Amatatongchai, M., Chairam, S., Kulsing, C., and Shen, W. (2016) Chromatic analysis by monitoring unmodified silver nanoparticles reduction on double layer microfluidic paper-based analytical devices for selective and sensitive determination of mercury(II). *Talanta*, 155:193–201.
82. Moonrungssee, N., Pencharee, S., and Jakmunee, J. (2015) Colorimetric analyzer based on mobile phone camera for determination of available phosphorus in soil. *Talanta*, 136:204–209.
83. García, A., Erenas, M. M., Marinetto, E. D., Abad, C. A., De Orbe-Paya, I., Palma, A. J., and Capitán-Vallvey, L. F. (2011) Mobile phone platform as portable chemical analyzer. *Sens. Actuators B*, 156:350–359.
84. Yakoh, A., Rattanarat, P., Siangproh, W., and Chailapakul, O. (2018) Simple and selective paper-based colorimetric sensor for determination of chloride ion in environmental samples using label-free silver nanoprisms. *Talanta*, 178:134–140.

85. Guan, L., Tian, J., Cao, R., Li, M., Cai, Z., and Shen, W. (2014) Barcode-like paper sensor for smartphone diagnostics: An application of blood typing. *Anal. Chem.*, 86:11362–11367.
86. Park, Y. M., Han, Y. D., Kim, K. R., Zhang, C., and Yoon, H. C. (2015) An immunoblot-based optical biosensor for screening of osteoarthritis using a smartphone-embedded illuminometer. *Anal. Methods*, 7 (15):6437–6442.
87. Salles, M. O., Meloni, G. N., De Araujo, W. R., and Paixão, T R L C. (2014) Explosive colorimetric discrimination using a smartphone, paper device and chemometrical approach. *Anal. Methods*, 6:2047–2052.
88. Lopez-Ruiz, N., Curto, V. F., Erenas, M. M., Benito-Lopez, F., Diamond, D., Palma, A. J., and Capitan-Vallvey, L F. (2014) Smartphone-based simultaneous pH and nitrite colorimetric determination for paper microfluidic devices. *Anal. Chem.*, 86:9554–9562.
89. Sicard, C., Glen, C., Aubie, B., Wallace, D., Jahanshahi-Anbuhi, S., Pennings, K., Daigger, G. T., Pelton, R., Brennan, J. D., and Filipe, C. D., (2015) Tools for water quality monitoring and mapping using paper-based sensors and cell phones. *Water. Res.*, 70:360–369.
90. Dungchai, W., Chailapakul, O., and Henry, C S. (2009) Electrochemical detection for paper-based microfluidics. *Anal. Chem.*, 81:5821–5826.
91. Oh, J., and Chow, K. (2015) Recent developments in electrochemical paper-based analytical devices. *Anal. Methods*, 7:7951–7960.
92. Hasanzadeh, M., and Shadjou, N. (2016) Electrochemical and photoelectrochemical nano-immunesensing using origami paper based method. *Mater. Sci. Eng. C*, 61:979–1001.
93. Hu, C., Bai, X., Wang, Y., Jin, W., Zhang, X., and Hu, S. (2012) Inkjet printing of nanoporous gold electrode arrays on cellulose membranes for high-sensitive paper-like electrochemical oxygen sensors using ionic liquid electrolytes. *Anal. Chem.*,

84:3745–3750.

94. Dossi, N., Toniolo, R., Pizzariello, A., Impellizzieri, F., Piccin, E., and Bontempelli, G. (2013) Pencil-drawn paper supported electrodes as simple electrochemical detectors for paper-based fluidic devices. *Electrophoresis*, 34:2085–2091.
95. Godino, N., Gorkin, R., Bourke, K., and Ducree, J. (2012) Fabricating electrodes for amperometric detection in hybrid paper/polymer lab-on-a-chip devices. *Lab Chip*, 12:3281–3284.
96. Fosdick, S. E., Anderson, M. J., Renault, C., Degregory, P. R., Loussaert, J. A., and Crooks, R. M.. (2014) Wire, mesh, and fiber electrodes for paper-based electroanalytical devices. *Anal. Chem.*, 86:3659–3666.
97. Li, Z., Li, F., Hu, J., Wee, W. H., Han, Y. L., Pingguan-Murphy, B., Lu, T. J., and Xu, F. (2015) Direct writing electrodes using a ball pen for paper-based point-of-care testing. *Analyst*, 140:5526–5535.
98. Arduini, F., Micheli, L., Moscone, D., Palleschi, G., Piermarini, S., Ricci, F., and Volpe, G. (2016) Electrochemical biosensors based on nanomodified screen-printed electrodes: Recent applications in clinical analysis. *Trends Anal. Chem.*, 79:114–126.
99. Nantaphol, S., Chailapakul, O., and Siangproh, W. (2015) A novel paper-based device coupled with a silver nanoparticle-modified boron-doped diamond electrode for cholesterol detection. *Anal. Chim. Acta.*, 891:136–143.
100. Rungsawang, T., Punrat, E., Adkins, J., Henry, C., and Chailapakul, O. (2016) Development of electrochemical paper-based glucose sensor using cellulose-4-aminophenylboronic acid-modified screen-printed carbon electrode. *Electroanalysis*, 28:462–468.
101. Carvalha, R. F., Kfoury, M. S., Piazzetta, M. H. O., Gobbi, A. L., and Kubota, L. T. (2010) Electrochemical detection in a paper-based separation device. *Anal. Chem.*,

82:1162–1165.

102. Ge, S., Zhang, L., Zhang, Y., Liu, H., Huang, J., Yan, M., and Yu, J. (2015) Electrochemical K-562 cells sensor based on origami paper device for point-of-care testing. *Talanta*, 145:12–19.
103. Fan, L., Hao, Q., and Kan, X. (2018) Three-dimensional graphite paper based imprinted electrochemical sensor for tertiary butylhydroquinone selective recognition and sensitive detection. *Sens. Actuators. B*, 256:520–527.
104. Nunez-Bajo, E., Blanco-Lopez, M. C., Costa-Garcia, A., and Fernandez-Abedul, M. T. (2018) In situ gold-nanoparticle electrogeneration on gold films deposited on paper for non-enzymatic electrochemical determination of glucose. *Talanta*, 178:160–165.
105. Nie, Z., Deiss, F., Liu, X., Akbulut, O., and Whitesides, G. M. (2010) Integration of paper-based microfluidic devices with commercial electrochemical readers. *Lab Chip*, 10:3163–3169.
106. Wu, G., and Zaman, M H. (2015) Amperometric measurements of ethanol on paper with a glucometer. *Talanta*, 134:194–199.
107. Wang, C. C., Hennek, J. W., Ainla, A., Kumar, A. A., Lan, W. J., Im, J., Smith, B. S., Zhao, M., and Whitesides, G. M. (2016) A paper-based "pop-up" electrochemical device for analysis of beta-hydroxybutyrate. *Anal. Chem.*, 88:6326–6333.
108. Zhao, C., Thuo, M. M., and Liu, X. (2015) Corrigendum: A microfluidic paper-based electrochemical biosensor array for multiplexed detection of metabolic biomarkers. *Sci. Technol. Adv. Mater.*, 16:049501.
109. Fujimoto, T., Kawahara, S., Fuchigami, Y., Shimokawa, S., Nakamura, Y., Fukayama, K., Kamahori, M., and Uno, S. (2017) Portable electrochemical sensing system attached to smartphones and its incorporation with paper-based electrochemical glucose sensor. *International Journal of Electrical and Computer Engineering (IJECE)*, 7: 1423–1429.

110. Kawahara, S., Fuchigmami, Y., Shimokawa, S., Nakamura, Y., Kuretake, T., Kamahori, M., and Uno, S.. (2017) Portable electrochemical gas sensing system with a paper-based enzyme electrode. *TELKOMNIKA*, 15: 895–902.
111. Zhao, C., and Liu, X., (2016) A portable paper-based microfluidic platform for multiplexed electrochemical detection of human immunodeficiency virus and hepatitis c virus antibodies in serum. *Biomicrofluidics*, 10:024119.
112. Canovas, R., Parrilla, M., Blondeau, P., and Andrade, F J. (2017) A novel wireless paper-based potentiometric platform for monitoring glucose in blood. *Lab Chip*, 17:2500–2507.
113. Fan, Y., Liu, J., Wang, Y., Luo, J., Xu, H., Xu, S., and Cai, X. (2017) A wireless point-of-care testing system for the detection of neuron-specific enolase with microfluidic paper-based analytical devices. *Biosens. Bioelectron.*, 95:60–66.
114. Liang, L., Su, M., Li, L., Lan, F., Yang, G., Ge, S., Yu, J., and Song, X. (2016) Aptamer-based fluorescent and visual biosensor for multiplexed monitoring of cancer cells in microfluidic paper-based analytical devices. *Sens. Actuators. B*, 229:347–354.
115. Ueland, M., Blanes, L., Taudte, R. V., Stuart, B. H., Cole, N., Willis, P., Roux, C., and Doble, P. (2016) Capillary-driven microfluidic paper-based analytical devices for lab on a chip screening of explosive residues in soil. *J. Chromatogr. A*, 1436:28–33.
116. Wen, X., Wang, Q., and Fan, Z., (2018) Highly selective turn-on fluorogenic chemosensor for Zn(II) detection based on aggregation-induced emission. *Journal of Luminescence*, 194:366–373.
117. Anjana, R. R., Anjali Devi, J. S., Jayasree, M., Aparna, R. S., Aswathy, B., Praveen, G. L., Lekha, G. M., and Sony, G. (2018) S,n-doped carbon dots as a fluorescent probe for bilirubin. *Microchim. Acta*, 185: 1–11.
118. Wu, H., Yang, L., Chen, L., Xiang, F., and Gao, H. (2017) Visual determination of

ferric ions in aqueous solution based on a high selectivity and sensitivity ratiometric fluorescent nanosensor. *Anal. Methods*, 9:5935–5942.

1190. Das, P., and Krull, U. J. (2017) Detection of a cancer biomarker protein on modified cellulose paper by fluorescence using aptamer-linked quantum dots. *Analyst*, 142:3132–3135.

120. Zamora-Galvez, A., Morales-Narvaez, E., Romero, J., and Merkoci, A. (2018) Photoluminescent lateral flow based on non-radiative energy transfer for protein detection in human serum. *Biosens. Bioelectron.*, 100:208–213.

121. Zhang, D., Broyles, D., Hunt, E. A., Dikici, E., Daunert, S., and Deo, S K. (2017) A paper-based platform for detection of viral RNA. *Analyst*, 142:815–823.

122. Liang, L., Lan, F., Yin, X., Ge, S., Yu, J., and Yan, M. (2017) Metal-enhanced fluorescence/visual bimodal platform for multiplexed ultrasensitive detection of microRNA with reusable paper analytical devices. *Biosens. Bioelectron.*, 95:181–188.

123. Taudte, R. V., Beavis, A., Wilson-Wilde, L., Roux, C., Doble, P., and Blanes, L. (2013) A portable explosive detector based on fluorescence quenching of pyrene deposited on coloured wax-printed mupads. *Lab Chip*, 13:4164–4172.

124. Petrucci, J. F., and Cardoso, A. A., (2016) Portable and disposable paper-based fluorescent sensor for in situ gaseous hydrogen sulfide determination in near real-time. *Anal. Chem.*, 88:11714–11719.

125. Petryayeva, E., and Algar, W. R. (2013) Proteolytic assays on quantum-dot-modified paper substrates using simple optical readout platforms. *Anal. Chem.*, 85:8817–8825.

126. Guzman, J. M. C. C., Tayo, L. L., Liu, C-C., Wang, Y-N., and Fu, L-M. (2018) Rapid microfluidic paper-based platform for low concentration formaldehyde detection. *Sens. Actuators B*, 255:3623–3629.

127. Thom, N. K., Lewis, G. G., Yeung, K., and Phillips, S T. (2014) Quantitative

fluorescence assays using a self-powered paper-based microfluidic device and a camera-equipped cellular phone. *RSC Adv*, 4:1334–1340.

128. Song, Y. Z., Zhang, X. X., Ma, B., Wu, Z. Y., and Zhang, Z. Q. (2017) Performance of electrokinetic stacking enhanced paper-based analytical device with smartphone for fast detection of fluorescent whitening agent. *Anal. Chim. Acta*, 995:85–90.

129. Alahmad, W., Uraisin, K., Nacapricha, D., and Kaneta, T. (2016) A miniaturized chemiluminescence detection system for a microfluidic paper-based analytical device and its application to the determination of chromium (III). *Anal. Methods*, 8:5414–5420.

130. Liu, F., and Zhang, C. (2015) A novel paper-based microfluidic enhanced chemiluminescence biosensor for facile, reliable and highly-sensitive gene detection of *listeria monocytogenes*. *Sens. Actuators B*, 209:399–406.

131. Lebiga, E., Edwin Fernandez, R., and Beskok, A. (2015) Confined chemiluminescence detection of nanomolar levels of  $H_2O_2$  in a paper-plastic disposable microfluidic device using a smartphone. *Analyst*, 140:5006–5011.

132. Zangheri, M., Cevenini, L., Anfossi, L., Baggiani, C., Simoni, P., Di Nardo, F., and Roda, A. (2015) A simple and compact smartphone accessory for quantitative chemiluminescence-based lateral flow immunoassay for salivary cortisol detection. *Biosens. Bioelectron.*, 64:63–68.

133. Spyrou, E. M., Kalogianni, D. P., Tragoulias, S. S., Ioannou, P. C., and Christopoulos, T. K. (2016) Digital camera and smartphone as detectors in paper-based chemiluminometric genotyping of single nucleotide polymorphisms. *Anal. Bioanal. Chem.*, 408:7393–7402.

134. Gross, E. M., Durant, H. E., Hipp, K. N., and Lai, R. Y. (2017) Electrochemiluminescence detection in paper-based and other inexpensive microfluidic devices. *ChemElectroChem*, 4:1594–1603.



135. Delaney, J L. Hogan, C F. Tian, J. and Shen, W. (2011) Electrogenerated chemiluminescence detection in paper-based microfluidic sensors. *Anal. Chem.*, 83 :1300–1306.
136. Mani, V., Kadimisetty, K., Malla, S., Joshi, A. A., and Rusling, J. F. (2013) Paper-based electrochemiluminescent screening for genotoxic activity in the environment. *Environ. Sci. Technol.*, 47:1937–1944.
137. Doeven, E. H., Barbante, G. J., Kerr, E., Hogan, C. F., Endler, J. A., and Francis, P. S. (2014) Red-green-blue electrogenerated chemiluminescence utilizing a digital camera as detector. *Anal. Chem.*, 86:2727–2732.
138. Delaney, J. L., Doeven, E. H., Harsant, A. J., and Hogan, C. F. (2013) Use of a mobile phone for potentiostatic control with low cost paper-based microfluidic sensors. *Anal. Chim. Acta*, 790:56–60.
139. Chen, L., Zhang, C., and Xing, D. (2016) Paper-based bipolar electrode-electrochemiluminescence (BPE-ECL) device with battery energy supply and smartphone read-out: A handheld ECL system for biochemical analysis at the point-of-care level. *Sens. and Actuators B: Chem.*, 237:308–317.
140. Chen, M., Yang, H., Rong, L., and Chen, X. (2016) A gas-diffusion microfluidic paper-based analytical device ( $\mu$ PAD) coupled with portable surface-enhanced Raman scattering (SERS): Facile determination of sulphite in wines. *Analyst*, 141:5511–5519.
141. Villa, J. E., and Poppi, R. J. (2016) A portable SERS method for the determination of uric acid using a paper-based substrate and multivariate curve resolution. *Analyst*, 141:1966–1972.
142. Feng, S., Caire, R., Cortazar, B., Turan, M., Wong, A., and Ozcan, A. (2014) Immunochromatographic diagnostic test analysis using google glass. *ACS Nano*, 8:3069–3079.

## Figure Legends

Figure 1. Principles of the instrument-free detections in  $\mu$ PADs. (A) Time-readout, (B) Distance-readout, (C) Counting-readout, and (D) Text-readout. (A) and (D): Taken from Ref. 34 and 53, respectively. (B): Taken from Ref. 38.

Figure 2. Portable electrochemical analyzers. Commercial glucometer coupled with an E $\mu$ PAD, (B) Multichannel potentiostat for an E $\mu$ PAD, (C) Smartphone-based electrochemical detector, and (D) Data transfer system from the electrochemical device via Bluetooth. (A): Taken from Ref. 105. (B): Taken from Ref. 108. (C): Taken from Ref. 109. (D): Taken from Ref. 111 with permission of Institute of AIP Publishing.

- Glucose oxidase (Gox)
- Substrate
- Buffer containing  $\text{MgCl}_2$
- Phase-switching reagent (hydrophobic)
- Green dye

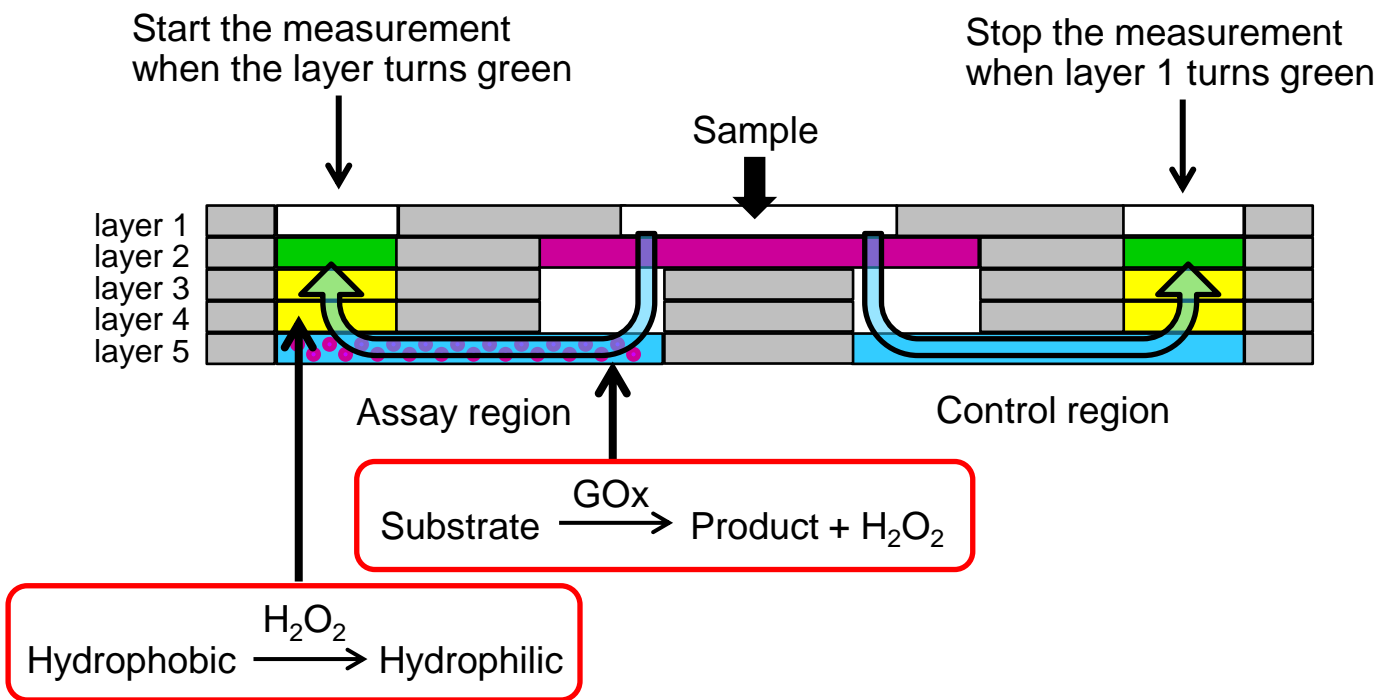


Figure 1 (A)

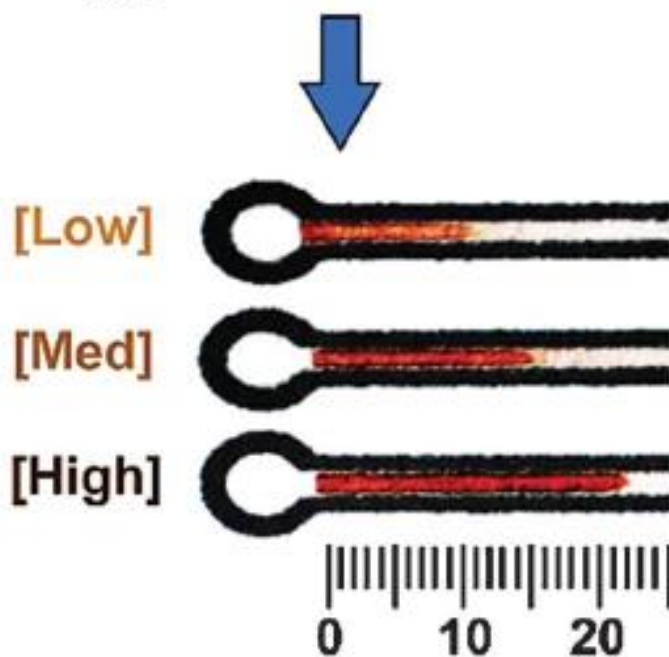
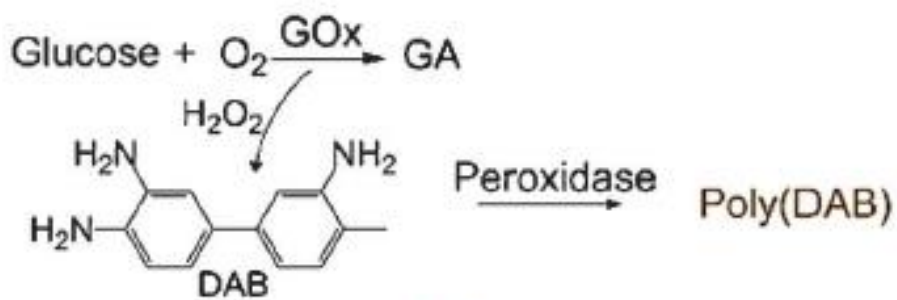
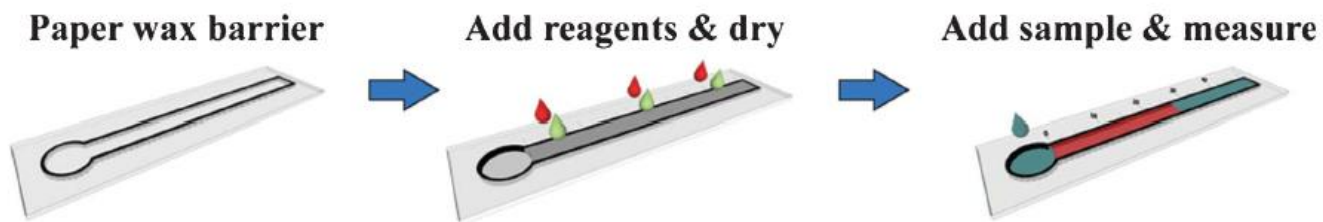
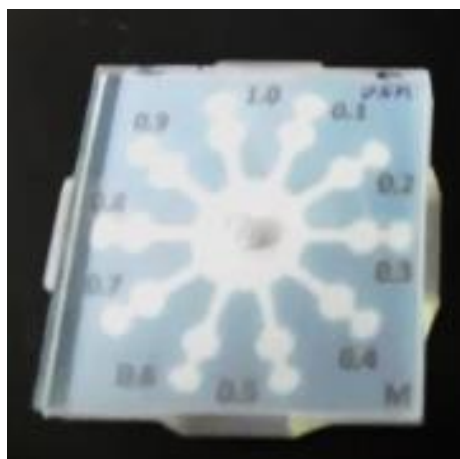
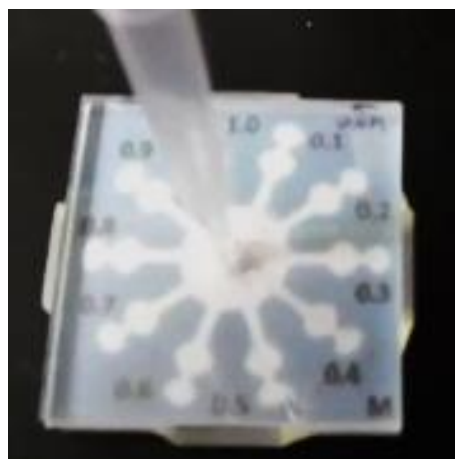


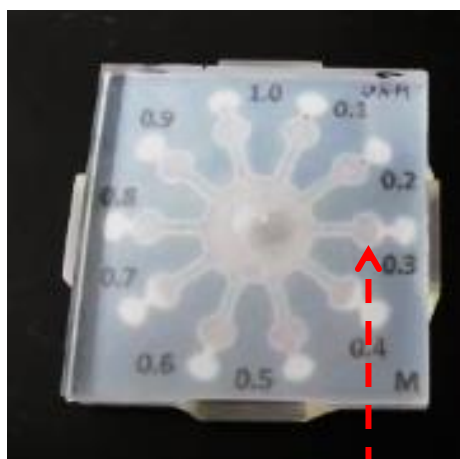
Figure 1 (B)



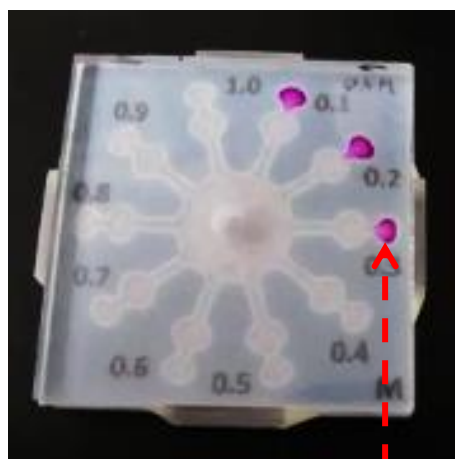
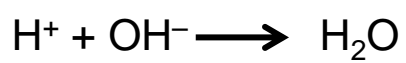
Before sample injection



Sample injection



Reaction



Detection

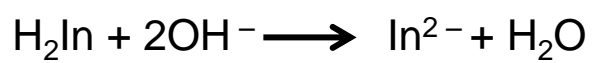


Figure 1 (C)

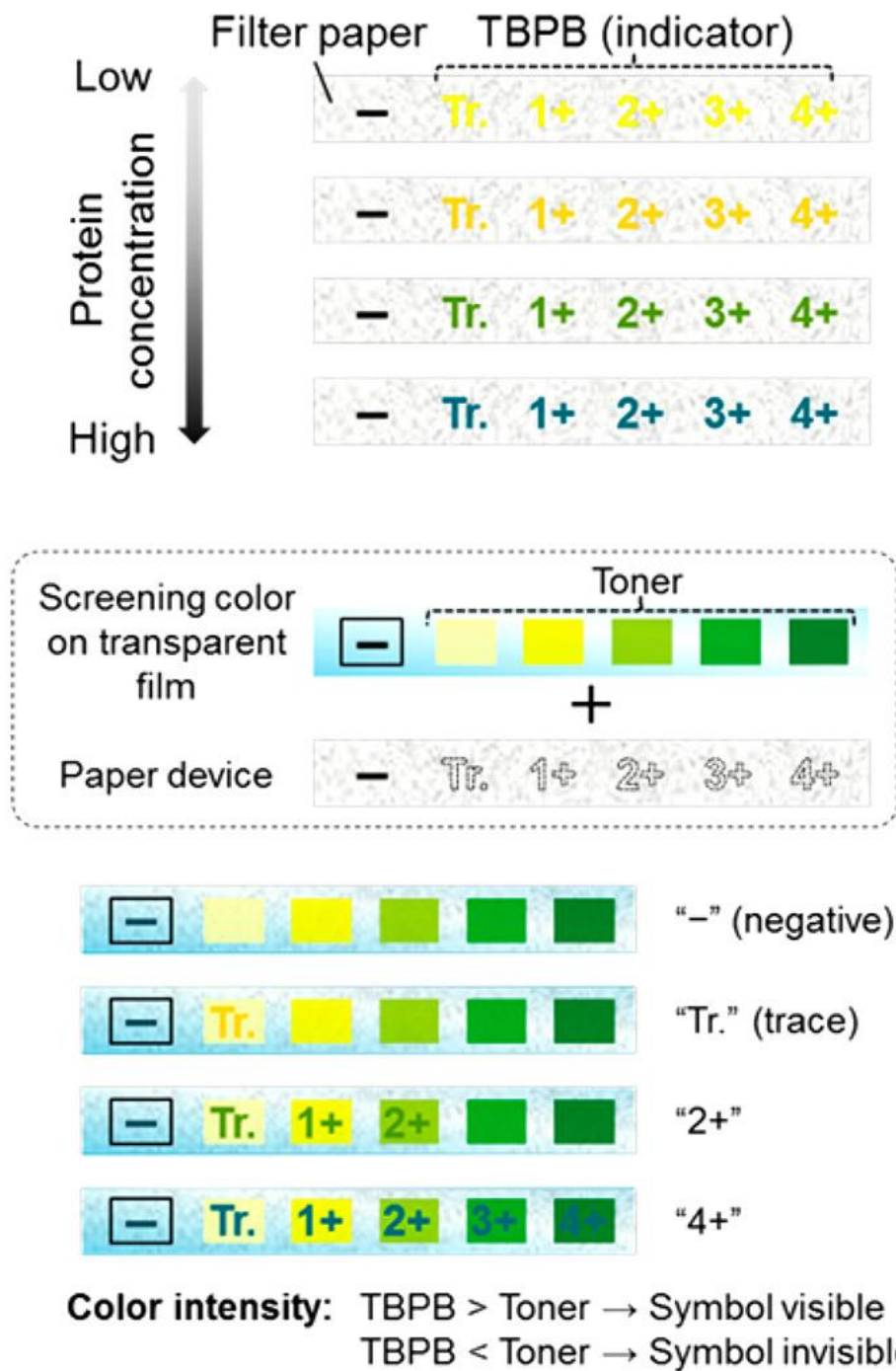


Figure 1 (D)

(A)



(B)

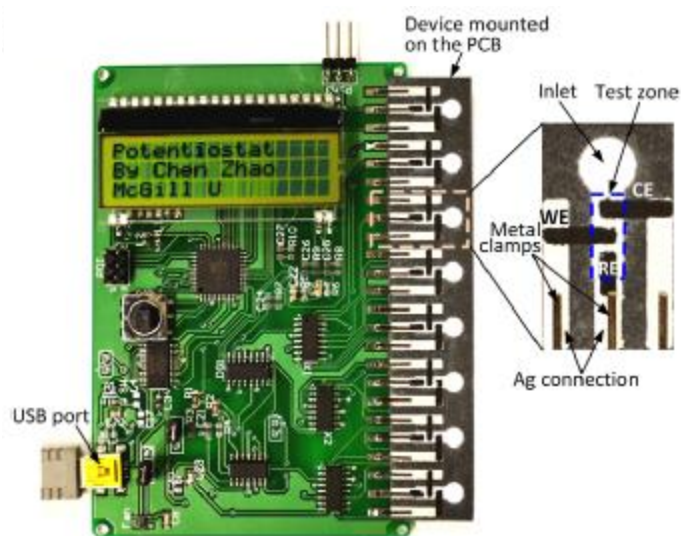
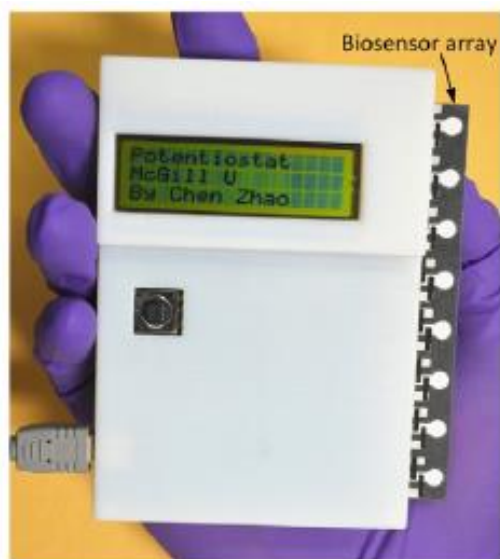
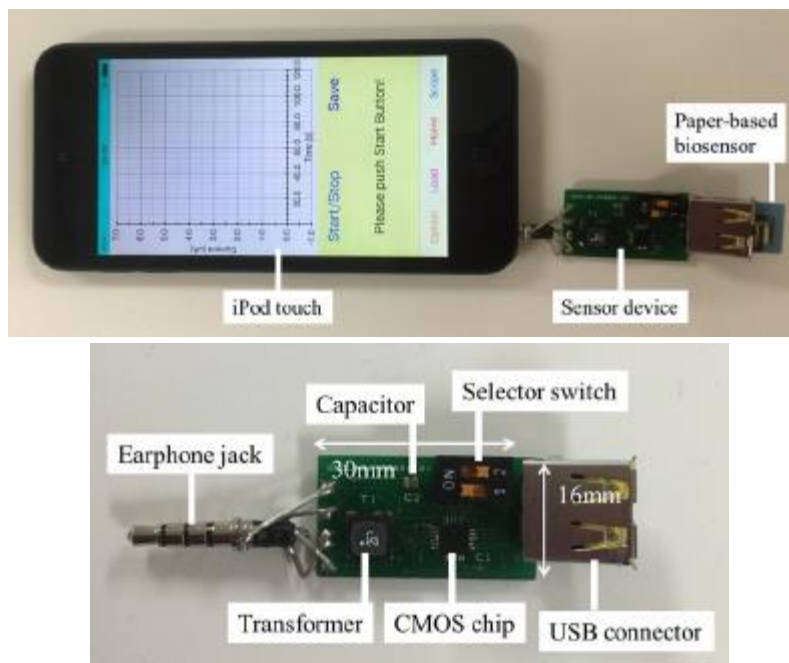


Figure 2

(C)



(D)

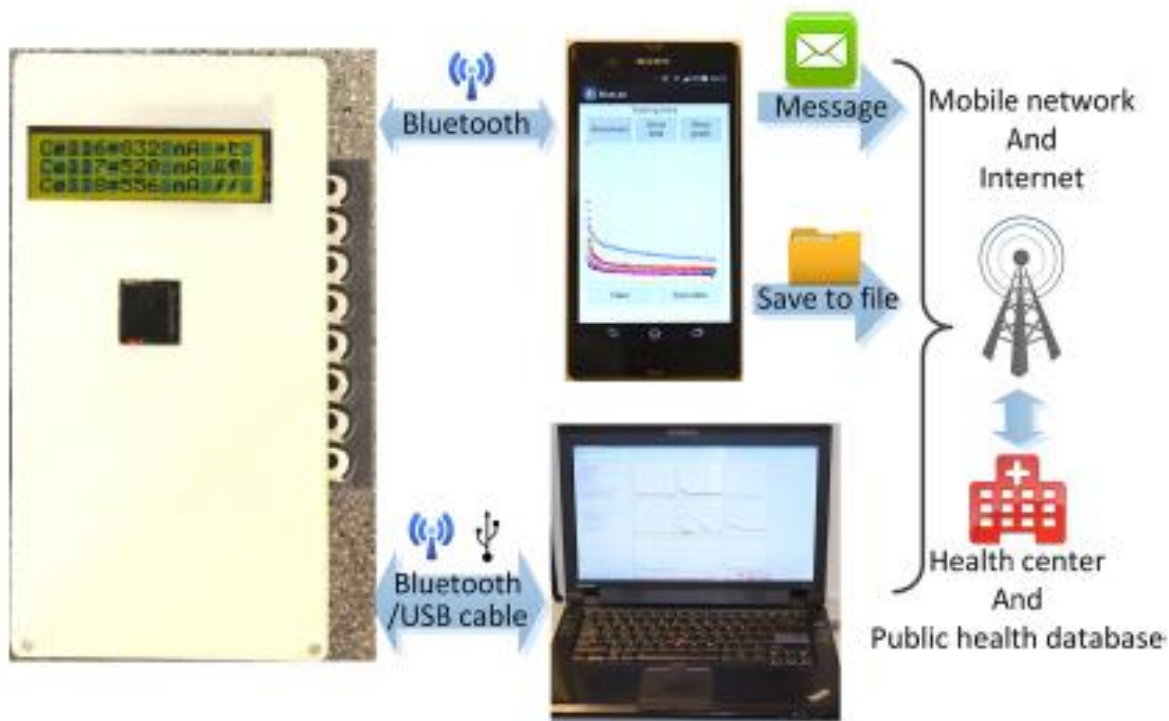
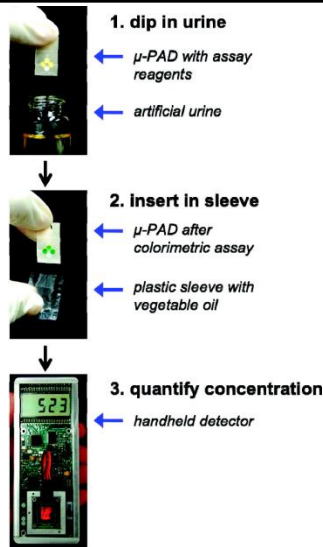
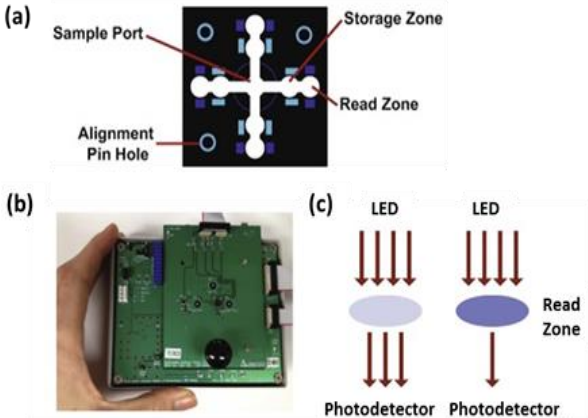
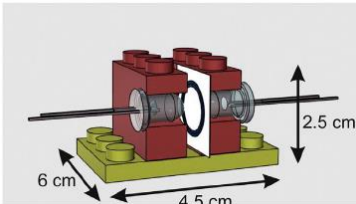
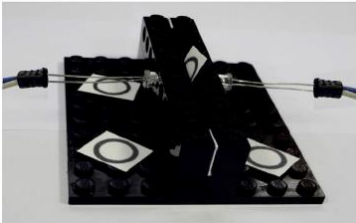
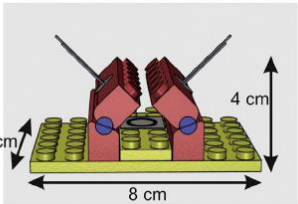



Figure 2



Table 1 Summary of transmittance colorimeters used with different  $\mu$ PADs and reaction system.

Analyte/Sample matrix	Reaction	Analytical features	Device image and description	Ref.
Bovine serum albumin (BSA)/Urine	Complex formation between BSA and tetrabromophenol blue	LR: 0-20 $\mu$ M LOD: (na) RSD: (na) $R^2$ : (na)	 <p>1. dip in urine ← <math>\mu</math>-PAD with assay reagents ← artificial urine</p> <p>2. insert in sleeve ← <math>\mu</math>-PAD after colorimetric assay ← plastic sleeve with vegetable oil</p> <p>3. quantify concentration ← handheld detector</p>	(57)
Alanine aminotransferase/ Blood	Enzymatic Reaction with Alanine transaminase, pyruvate oxidase, thiamine diphosphate, 4-aminoantipyrine, and N-ethyl-N-(2-hydroxy-3-sulfopropyl)-3,5-dimethoxyalanine	LR: 17-66 U L <sup>-1</sup> LOD: 6 U L <sup>-1</sup> RSD: (na) $R^2 = 0.924$	 <p>(a) Paper assay design.</p> <p>(b) Design of handheld portable reader.</p> <p>(c) An LED/PD pair surrounds the reading zone on each arm of the assay.</p>	(59)

Hemoglobin/ Human blood	Lysis of erythrocytes with sodium lauryl sulfate (sodium dodecyl sulfate)	LR: 0.5–30 g L <sup>-1</sup> LOD: 0.6 mg L <sup>-1</sup> RSD: (na) R <sup>2</sup> : (na)	<div data-bbox="894 37 1251 239">  </div> <div data-bbox="894 262 1251 482">  </div> <div data-bbox="894 496 1251 525">Transmittance measurement</div> <div data-bbox="1306 37 1605 239">  </div> <div data-bbox="1306 262 1605 482">  </div> <div data-bbox="1306 496 1605 525">Reflectance measurement</div>	(60)
----------------------------	---	---	--	------

LR: Linear range, LOD: Limits of detection, RSD: Relative standard deviation, R<sup>2</sup>: Correlation coefficient.

Taken from Ref. 57. Taken from Ref. 59. Taken from Ref. 60 with permission of Elsevier. .